

Nanostructures

Actinyl Peroxide Nanospheres**

Peter C. Burns, Karrie-Ann Kubatko, Ginger Sigmon,
Brian J. Fryer, Joel E. Gagnon, Mark R. Antonio, and
L. Soderholm*

Self-assembling small clusters provide an ideal venue for the study of fundamental structure–property relationships. The monodispersed nanoaggregates that have been reported to

[*] Prof. P. C. Burns, K.-A. Kubatko, G. Sigmon
Department of Civil Engineering and Geological Sciences
University of Notre Dame
156 Fitzpatrick Hall, Notre Dame, IN 46556 (USA)
Fax: (+1) 574-631-9236
E-mail: pburns@nd.edu
Prof. Dr. B. J. Fryer, J. E. Gagnon
Great Lakes Institute for Environmental Research
University of Windsor
Windsor, Ontario N9B 3P4 (Canada)
Dr. M. R. Antonio, Dr. L. Soderholm
Chemistry Division
Argonne National Laboratory
Argonne, IL 60439 (USA)

[**] This research was supported at the University of Notre Dame by the Environmental Management Science Program of the Office of Science, US Department of Energy (DE-FG07-97ER14820), and the National Science Foundation Environmental Molecular Science Institute at the University of Notre Dame (EAR02-21966). This research was supported at Argonne National Laboratory by the US Department of Energy Office of Basic Energy Sciences (DOE/BES) – Chemical Sciences Division and by the Material Sciences Division for the Advanced Photon Source studies under contract number W-31-109-ENG-38.

date are based on main-group elements, most notably C_{60} (buckminsterfullerene)^[1] and transition-metal oxide clusters, including a wide variety of polyoxometalates built on WO, MoO, and NbO frameworks.^[2] Studies based on these systems have resulted in new insight into electronic, magnetic, and structural properties at the nanoscale and provide numerous examples of novel materials with important applications.^[3,4] Nanoparticles are also of considerable importance in many environmental systems as they often form at low temperatures, can impact the transport of heavy metals and radionuclides in geologic fluids, and are small enough that their properties are often particle-size dependent.^[5] Herein, we report the synthesis and characterization of a new family of self-assembling nanospheres from actinide ions (Ac) and their persistence as stable entities in alkaline solutions. These nanospheres have compositions such as $[K_{16}(H_2O)_2(UO_2)(O_2)_2(H_2O)_2\{(UO_2)(O_2)_{1.5}\}_{28}]^{14-}$ and $[Li_6(H_2O)_8NpO_2(H_2O)_4\{(NpO_2)(O_2)(OH)\}_{24}]^{20-}$ and are comprised of linear actinyl peroxide building blocks.

The uranyl and neptunyl members of this new family of actinyl peroxide compounds precipitated from alkaline peroxide solutions of U^{VI} and Np^{VI} ions at 25 °C after approximately seven days or longer. Figure 1 a–c shows the struc-

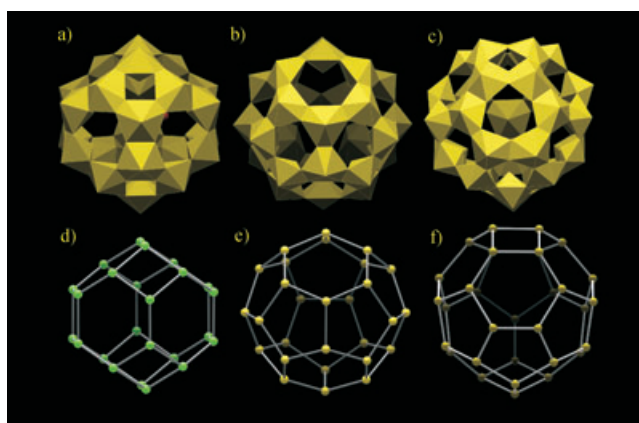


Figure 1. Polyhedral representations of spherical actinyl peroxide nanoclusters found in a) U-24 and Np-24, b) U-28, and c) U-32 and Ac–Ac connectivity diagrams for d) Np-24, e) U-28, and f) U-32.

tures of four exemplary actinyl peroxide nanospheres that are the focus herein. Their molecular units are composed of 24, 28, or 32 uranyl peroxide polyhedra (U-24, U-28, and U-32) or 24 neptunyl peroxide polyhedra (Np-24).^[6] The nanospheres are approximately 16.4, 17.7, and 18.6 Å in diameter (as measured between the centers of bonding oxygen atoms).

The nanospheres are composed of two types of actinyl peroxide polyhedra: U-24, U-32, and Np-24 contain topologically identical $[(AcO_2)(O_2^{2-})_2(OH)_2]$ hexagonal bipyramids, in which the oxygen atoms of the actinyl ions constitute the apices of the bipyramids and the peroxide groups form two of the equatorial edges of the polyhedra (Figure 1 a,c). U-28 contains only $[(AcO_2)(O_2^{2-})_3]$ hexagonal bipyramids, in which three equatorial edges of the polyhedra are peroxide groups (Figure 1 b). In all cases, the hexagonal bipyramids are linked by sharing three of their equatorial edges with adjacent

polyhedra. Two of the shared edges in U-24, Np-24, and U-32 correspond to peroxide groups and the third edge consists of two hydroxy groups, whereas all three shared edges in U-28 are peroxide groups. The outer surfaces of the nanospheres are the oxygen atoms of the actinyl ions and each $Ac^{VI}-O$ bond corresponds to approximately 1.7 valence units;^[7] therefore, these oxygen atoms can form only weak bonds.

The shortening of the polyhedra edges associated with peroxide groups favors formation of nanospheres over the normal linkage into sheets or chains. Figure 2 illustrates the

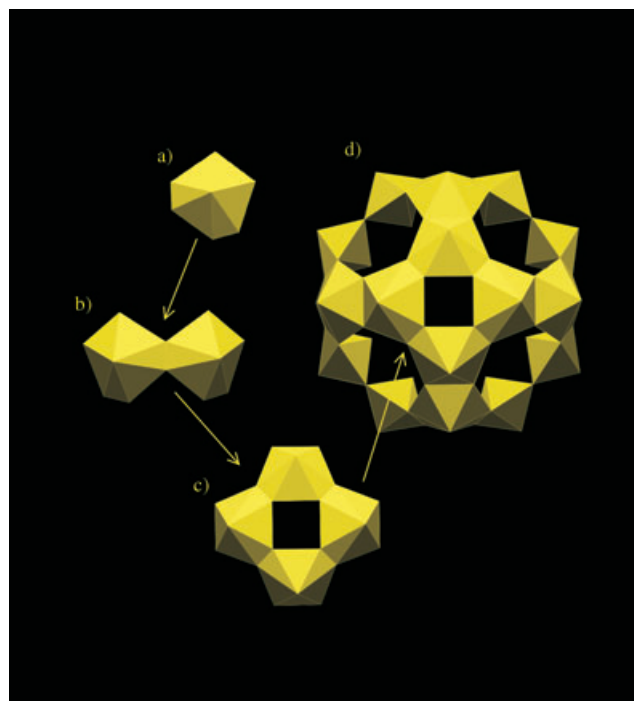


Figure 2. Polyhedral representations of linkages in the U-24 and Np-24 nanoclusters: a) hexagonal bipyramid with composition $[(AcO_2)(O_2)_2(OH)_2]$, b) linkages of two hexagonal bipyramids by the sharing of a peroxide edge, c) linkage of four hexagonal bipyramids into a four-membered ring by the sharing of four peroxide edges, and d) the U-24 cluster.

linkage of the polyhedra into four-membered rings in U-24, U-32, and Np-24. Each shared edge within the four-membered ring is a peroxide group with approximate lengths of 1.45 Å, whereas the edge defined by one oxygen atom of each of the two peroxide groups has a length of approximately 2.8 Å. The linkage of four polyhedra into a ring requires a tilting of the polyhedra with the actinyl ions directed towards a common point located approximately 3.5 Å below the four coplanar Ac^{VI} cations (Figure 2 c). The nanospheres found in U-24 and Np-24 result from the linkage of eight topologically and chemically identical four-membered rings of polyhedra (Figure 2 d).

U-28 contains 28 uranyl triperoxide polyhedra that form the nanosphere, and there is a partially occupied $[(UO_2)(O_2)_2(H_2O)_2]$ polyhedron at its center (Figure 3 b). There are 16 K-ion sites within the cluster that bond to as many as ten ligands, which are mostly at the vertices of the uranyl

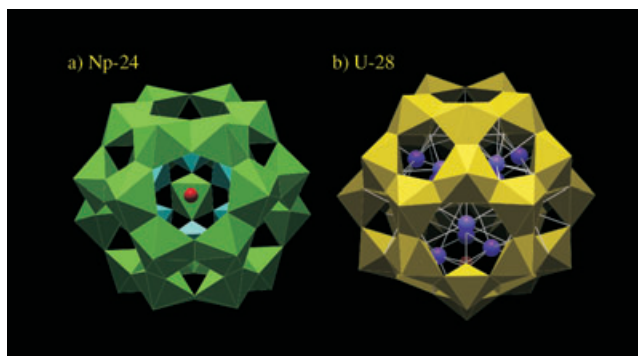


Figure 3. Polyhedral representations of the details of the a) Np-24 and b) U-28 clusters. $[\text{NpO}_2(\text{O}_2)_2(\text{OH})_2]$ polyhedra are green, $[\text{UO}_2(\text{O}_2)_3]$ polyhedra are yellow, LiO_5 polyhedra are blue, K cations are shown as purple spheres, and O atoms of the H_2O groups are shown as red spheres in (b).

polyhedra. In the case of occupancy of the U position at the center of the cluster, the composition is $[\text{K}_{16}(\text{H}_2\text{O})_2(\text{UO}_2)(\text{O}_2)_2(\text{H}_2\text{O})_2(\text{UO}_2)(\text{O}_2)_{1.5}]_{28}^{14-}$. The charge of the nanosphere in each structure is balanced by Li or K ions in the intercluster regions. The Li-ion content was confirmed for U-24 by laser-ablation inductively coupled plasma mass spectrometry (ICPMS) and was 1.90 ± 0.15 wt %, which is comparable to the theoretical value of 1.77 wt %, which was derived from the U/Li ion ratio of 1:1 required for charge balance.

Np-24 and U-28 also contain an actinyl ion at the center of the nanosphere, although these sites are occupied in approximately 50 % of the clusters and are not necessary for their stability. U-24, Np-24, and U-32 contain Li ions and H_2O , while U-28 contains K ions and H_2O . The actinyl ion at the center of Np-24 is in square bipyramidal coordination with four equatorial H_2O groups, and each of the ligands are shared with LiO_5 square pyramids (Figure 3a). The framework of Np-24 contains four symmetrically independent Np sites: each center has a neptunyl ion with Np–O bond lengths of 1.792(11) and 1.809(9) Å for Np1, 1.802(10) and 1.839(10) Å for Np2, 1.784(7) and 1.811(7) for Np3, and 1.788(7) and 1.796(7) Å for Np4. The equatorial Np–O bond lengths range from 2.344 to 2.455 Å for all polyhedra, and the average equatorial Np–O bond lengths are 2.407, 2.433, 2.389, and 2.382 Å for Np1, Np2, Np3, and Np4, respectively. The neptunyl ion geometry and the equatorial Np–O bond lengths indicate that Np1, Np3, and Np4 are hexavalent, whereas the longer neptunyl and equatorial bond lengths for Np2 strongly suggest it is pentavalent. The valence of the Np5 ion at the center of the nanosphere is ambiguous, but it is present as an actinyl ion and is considered hexavalent for the purpose of counting charges. Np-24 also contains eight H_2O groups, which are only held in place by hydrogen-bonding interactions. Where the Np site at the center of Np-24 is occupied, its composition is $[\text{Li}_6(\text{H}_2\text{O})_8\text{NpO}_2(\text{H}_2\text{O})_4(\text{NpO}_2)(\text{O}_2)(\text{OH})]_{24}^{20-}$.

The crystals of all of the U-based nanospheres are yellow, which is consistent with the $(\text{UO}_2)^{2+}$ ion and its unoccupied valence f states.^[8] Most cluster anions based on W–O, Mo–O, and Nb–O units are white and have unoccupied valence

d states. In contrast, the crystals of the neptunyl nanospheres are close to black and are composed primarily of Np^{VI} , which are f¹ ions. Np2 is of further interest as the Np–O bond lengths indicate it is an Np^{V} ion. The slight difference in the coordination environment of this site relative to the other Np^{VI} sites in the framework suggests that Np-24 may be electroactive under a minimal applied potential, which is similar to the behavior exhibited by several polyoxometalates based on W–O groups.^[9–11]

Small angle X-ray scattering (SAXS) data for solutions of H_2O_2 , LiOH, and $[\text{UO}_2(\text{NO}_3)_2(\text{H}_2\text{O})_6]$ in H_2O recorded 2, 28, and 180 days following their initial preparation are shown together with the fitted response in Figure 4. The time

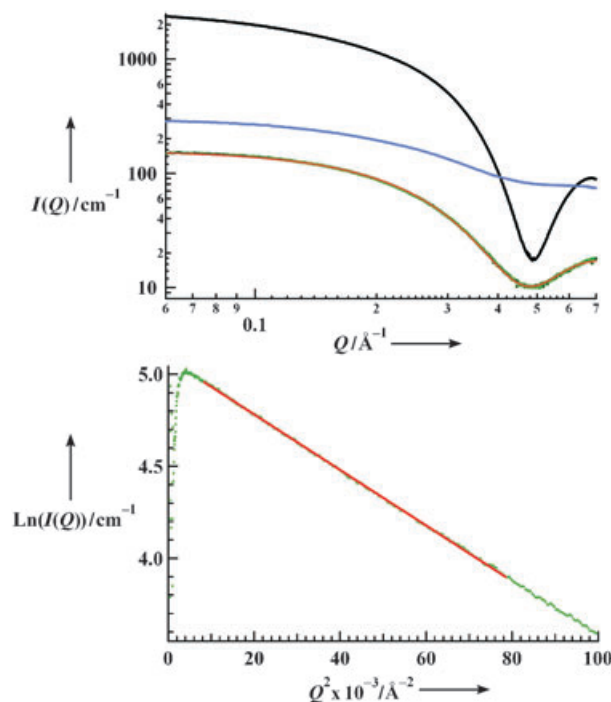


Figure 4. SAXS data from the mother liquor (H_2O , H_2O_2 , LiOH, and $[\text{UO}_2(\text{NO}_3)_2(\text{H}_2\text{O})_6]$) 2 (blue line), 28 (black line), and 180 days (green line) old. Top: change in the shape of the curves with solution age demonstrates evolving aggregation of the uranyl species. Data for the solutions after 2 and 28 days indicate the presence of multiple aggregates. Data for the solutions after 180 days are consistent with a spherical-shell model (red line), thus indicating a monodisperse cluster in solution. Bottom: Guinier plot of data for the solution after 180 days, which is linear over a wide Q range and so is a representative fit (red line, ca. $0.01\text{--}0.03 \text{ Å}^{-2}$).

progression of the scattering data, particularly for the high Q data that deepen and broaden with sample age, are attributed to an evolving distribution both in terms of size and morphology of uranyl peroxo aggregates in solution. The data obtained from the solution aged for 180 days, which produced U-24 crystals, corresponds to spherically ripened monodisperse nanospheres. There are indications of cluster anion polydispersity in the SAXS data for the two younger solutions. A spherical-shell model provided the best fit of the $I(Q)$ versus Q data from the solution recorded after 180 days

and was in excellent agreement with the solid-state structural data. The central cavity radius determined by the spherical-shell model was 1.7 ± 0.2 Å and the shell radius was 6.2 ± 0.2 Å, which represents an overall diameter of 16.2 Å. Confirmation for the presence of well-formed U-24 nanospheres in solution was obtained from a Guinier analysis of the low- Q SAXS data. A radius of gyration ($R_g = 6.7 \pm 0.1$ Å), determined from the fit to the low- Q data (Figure 4), was the same (within error) as the R_g value determined from the U-24 single-crystal structural parameters.

The SAXS data reveal an evolving structural organization in solution with well-defined clusters present as early as two days after preparation. The overall change in SAXS data with time indicates a ripening of the solution and is consistent with a self-assembly process that yields the initial nanospheres in solution, which subsequently precipitated. This mechanism is consistent with the lag time of several days between the initial preparation of the solution and precipitation of the nanospheres. Verification of the existence and solubility of U-24 in solution as a stable anionic species suggests a variety of further synthetic, structural, magnetic, electrochemical, and reactivity studies.

The actinyl peroxide nanospheres described herein represent a new class of polyoxometalates. The largest reported actinide polyoxometalate ion to date contains only six U^V ions.^[12] Only 41 out of over 325 inorganic structures known to contain essential U^VI ions have finite clusters of polyhedra composed of high-valence cations,^[13] and none contain more than four uranyl polyhedra. Peroxopolyoxometalates that contain Mo, W, and V form in aqueous solutions in the presence of small quantities of H_2O_2 and some catalyze the oxidation of a variety of organic substrates with H_2O_2 as the cooxidant.^[14–16] Several such peroxopolyoxometalates have been isolated and structurally characterized.^[17] The peroxide group typically defines an outer edge of a polyhedron in such clusters, although one or both of the oxygen atoms of the peroxide group form a bridge between metal centers in some cases.^[18] Peroxo groups occur along the shared edges of the uranyl polyhedra in the nanospheres isolated in the current study and are, therefore, integral elements of the structure connectivity.

The formation of actinyl peroxide nanospheres is important from a practical standpoint, as they may form in alkaline mixtures of nuclear waste containing various salts and organic solvents by incorporating peroxides created by the alpha-radiolysis of water. The synthesis conditions reported herein are broadly similar to those in high-level waste storage tanks (for example, alkaline solution, ambient temperature),^[19,20] as well as soils and sediments contaminated by the leakage of such waste. The formation of actinyl peroxide nanospheres in such systems is probable and could have a profound impact on the mobility of actinides in the environment given their persistence in solution.

This new class of actinyl peroxide clusters is a rare example of self-assembling nanospheres. The potential for the further preparation of novel structure types through the metered addition of actinyl peroxide units is suggested by solution SAXS data and is demonstrated by the variety of structures synthesized. A series of structurally tuneable

spheroids would afford an unprecedented opportunity to study size/structure–function relationships. Furthermore, variability in the valence electron count associated with the actinyl ions, coupled with 5f-bonding behavior that is intermediate between localized and itinerant, offers the control to systematically probe electronic, magnetic, and catalytic properties on the nanoscale. The broad potential generated by the tunability of the actinyl peroxides and their likely presence in natural and contaminated environmental samples provides impetus for further study of this unusual family of nanospheres.

Experimental Section

Crystals of U-24, U-28, U-32, and Np-24 were obtained from alkaline solutions left to stand at 298 K in air for 7–14 days. The solutions contained the following: U-24: 30% H_2O_2 (5 mL), H_2O (1 mL), LiOH (1 g), 3M $[UO_2(NO_3)_2(H_2O)_6]$ solution in H_2O (1 mL); U-28: aqueous solution of tartaric acid (0.1 mL), 4M KOH in H_2O (0.25 mL), 30% H_2O_2 (0.15 mL), 3M $[UO_2(NO_3)_2(H_2O)_6]$ solution in H_2O (0.25 mL); U-32: 30% H_2O_2 (1 mL), H_2O (1 mL), LiOH (1 g), 3M solution of $[UO_2(NO_3)_2(H_2O)_6]$ in H_2O (1 mL); Np-24: 87 mM Np^V ions in 1M HCl (1 mL), 30% H_2O_2 (0.04 mL), 2M LiOH solution in H_2O (1.38 mL). The syntheses for U-24, U-32, and Np-24 each provided several dozen crystals as well as fine-grained precipitates. The yields were estimated to be 20–40%. The synthesis of U-28 provided only one identifiable crystal.

The laser-ablation ICPMS analysis of U-24 crystals was conducted at the Great Lakes Institute for Environmental Research, University of Windsor with a nonhomogenized, solid-state, 266 nm Nd-doped Y–Al garnet (Nd/YAG) laser. Sample ablation was done in a sampling cell filled with argon gas on a modified polarizing microscope. Ablated material was transported in an argon carrier gas from the ablation cell to the ICPMS equipment. The U-24 crystals were mounted on double-sided tape attached to precleaned glass microscope slides and were traversed into the laserbeam using a computer-controlled X–Y–Z stage. The normal high sensitivity (ppb to low ppm) of the analytical system was reduced by positioning a $2.5 \times$ beam expander in front of a 1.0 mm pinhole in the laser path prior to focusing the laser energy on the sample. The vastly different elemental concentrations of the calibration standard and U-24 were compensated for by decreasing the laser power between the NIST glass (1.30 kV) and U-24 (1.20 kV) ablations.

The Li content was analyzed on a ThermoElemental X-7 ICP mass spectrometer. NIST glass standard 610 was used for calibration with elemental uranium as the internal standard (NIST 610 = 457 ppm and U-24 = 60.64 wt % U, respectively). The absolute sensitivity of the Li content (relative to elemental uranium) was increased by addition of ultrapure nitrogen gas at a flow rate of 3.0 mL min^{-1} to the nebulizer gas flow downstream of the laser cell. The LAM-TRACE program^[21] was used to convert the ICPMS output data (integrated counts/second) into concentration units.

The SAXS data were collected with the facilities at beam-line 12-BM-B at the Advanced Photon Source.^[22] An incident photon energy of 16 keV was chosen to eliminate X-ray fluorescence that is excited by higher-energy incident photons at (and above) the $U L_{3\text{-edge}}$ threshold of 17.166 keV. Approximately 20 μL of the cluster-containing solutions were contained in purpose-built polychlorotrifluoroethylene (PCTFE), thin-layer cells with 0.010" PCTFE windows and a 1.7 mm pathlength. Data reduction to obtain $I(Q)$ versus Q (\AA^{-1}), where $Q = 4\pi \sin \theta / \lambda$ and 2θ is the scattering angle and λ is the wavelength of the X-rays, was performed following standard procedures, and Guinier analysis in the low Q region was carried out using

standard methods to obtain the radius of gyration R_g of the particles.^[23,24]

Received: October 27, 2004

Keywords: actinides · peroxides · polyoxometalates · self-assembly · uranium

- [1] H. W. Kroto, J. R. Heath, S. C. O'Brien, R. F. Curl, R. E. Smalley, *Nature* **1985**, 318, 162.
- [2] A. Muller, F. Peters, M. T. Pope, D. Gatteschi, *Chem. Rev.* **1998**, 98, 239.
- [3] A. F. Hebard, M. J. Rosseinsky, R. C. Haddon, D. W. Murphy, S. H. Glarum, T. T. M. Palstra, A. P. Ramirez, A. R. Kortan, *Nature* **1991**, 350, 600.
- [4] "Comprehensive Coordination Chemistry-II: From Biology to Nanotechnology": C. L. Hill in *Applications of Coordination Chemistry*, Vol. 4 (Ed.: M. Ward), Elsevier, Oxford, **2003**, pp. 679–759.
- [5] J. F. Banfield, H. Zhang, *Rev. Mineral. Geochem.* **2001**, 44, 1.
- [6] X-ray diffraction data for U-24, U-28, and U-32 were collected at 100 K using a Bruker SMART APEX diffractometer at the University of Notre Dame ($\lambda = 0.71073$ Å). X-ray diffraction data for Np-24 was collected at 298 K using a Bruker SMART APEX II diffractometer at Argonne National Laboratory ($\lambda = 0.71073$ Å). A sphere of data was collected for each crystal using frame-widths of 0.3° in ω . Data were corrected for Lorentz and polarization using the Bruker program SAINT, absorption corrections were performed using the Bruker program XPREF (version 5.1, 1997), and the structures were solved by direct methods and refined on the basis of F^2 for all unique reflections using the Bruker SHELXTL system of programs (version 5.10, 1997). Refinement of the structure of Np-24 was straightforward. The Np5 site, located at the center of the nanosphere, and its associated ligands were assigned 50% occupancy following refinement of their corresponding site occupancies. Refinement of the structure of U-24 was challenging because of the very large number of atoms in the asymmetric unit and the contrast of scattering efficiencies between the Li and U atoms. Soft constraints of Li–O distances were added to the refinement, and the positions of the Li atoms are tentative. Refinement of the structure of U-28 was reasonably straightforward: Following refinement of their scattering site, the occupancies of U18, which is located at the center of the nanosphere, and its associated oxygen atoms were set at 50%. The K atoms in the structure were assigned full occupancy, but some may be partially occupied by K atoms or a combination of K atoms and H₂O. Solution of U-32 and refinement of its structure was extremely difficult because of the large number of atoms in the asymmetric unit and positional disorder of some constituents. Soft constraints for U–O(uranyl) distances were added to the refinement to improve the uranyl ion geometries. It was not possible to locate any Li atoms in the structure, and the positions and identities of oxygen atoms not bonded to U atoms are considered to be tentative. U-24: 315223 total reflections, 75761 unique reflections, 75761 reflections used in the refinement, 26.6° maximum theta, $R1 = 0.080$, $wR2 = 0.186$, GOF = 0.80, space group $P\bar{1}$, triclinic, $a = 19.2111(11)$, $b = 31.003(2)$, $c = 32.252(2)$ Å, $\alpha = 102.404(4)$, $\beta = 99.506(4)$, $\gamma = 95.362(4)^\circ$, $V = 18336.8(19)$ Å³. Np-24: 46131 total reflections, 5606 unique reflections, 5606 reflections used in the refinement, 28.3° maximum theta, $R1 = 0.044$, $wR2 = 0.122$, GOF = 1.04, space group $I4/m$, tetragonal, $a = 18.1554(4)$, $c = 26.6926(14)$, $V = 8798.4(5)$ Å³. U-28: 140070 total reflections, 12294 unique reflections, 12294 reflections used in the refinement, 22.5° maximum theta, $R1 = 0.058$, $wR2 = 0.141$, GOF = 0.75, space group $Pbcm$, orthorhombic, $a = 19.2609(13)$, $b = 33.813(2)$, $c = 28.1628(19)$ Å, $V = 18341(2)$ Å³. U-32: 275074 total reflections, 74664 unique reflections, 74664 reflections used in the refinement, 22.5° maximum theta, $R1 = 0.085$, $wR2 = 0.153$, GOF = 0.52, space group $P2_1/c$, monoclinic, $a = 38.84(3)$ Å, $b = 36.52(3)$ Å, $c = 41.30(3)$ Å, $\beta = 102.863(13)^\circ$, $V = 57098(69)$ Å³. Further details on the crystal structure investigations may be obtained from the Fachinformationszentrum Karlsruhe, 76344 Eggenstein-Leopoldshafen, Germany (fax: (+49) 7247-808-666; e-mail: crysdata@fiz-karlsruhe.de) on quoting the depository number CSD-414640 (U-24), -414641 (Np-24), -414642 (U-28), and -414643 (U-32).
- [7] P. C. Burns, R. C. Ewing, F. C. Hawthorne, *Can. Mineral.* **1997**, 35, 1551.
- [8] R. G. Denning, *Struct. Bonding (Berlin)* **1992**, 79, 215.
- [9] D. C. Duncan, C. L. Hill, *Inorg. Chem.* **1996**, 35, 5828.
- [10] B. Keita, Y. Jean, B. Levy, L. Nadjo, R. Contant, *New J. Chem.* **2002**, 26, 1314.
- [11] M.-H. Chiang, M. R. Antonio, L. Soderholm, *Dalton Trans.* **2004**, 3562.
- [12] P. B. Duval, C. J. Burns, D. L. Clark, D. E. Morris, B. L. Scott, J. D. Thompson, E. L. Werkema, L. Jia, R. A. Andersen, *Angew. Chem.* **2001**, 113, 3461; *Angew. Chem. Int. Ed.* **2001**, 40, 3358.
- [13] P. C. Burns, *Mater. Res. Soc. Symp. Proc.* **2004**, 802, 89.
- [14] P. Gouzerh, A. Proust, *Chem. Rev.* **1998**, 98, 77.
- [15] D. C. Duncan, R. C. Chambers, E. Hecht, C. L. Hill, *J. Am. Chem. Soc.* **1995**, 117, 681.
- [16] M. V. Vasylyev, R. Neumann, *J. Am. Chem. Soc.* **2004**, 126, 884.
- [17] D. Sloboda-Rozner, P. L. Alsters, R. Neumann, *J. Am. Chem. Soc.* **2003**, 125, 5280.
- [18] M. H. Dickman, M. T. Pope, *Chem. Rev.* **1994**, 94, 569.
- [19] B. Wakoff, K. L. Nagy, *Environ. Sci. Technol.* **2004**, 38, 1765.
- [20] B. O. Hansen, P. Kwan, M. M. Benjamin, C.-W. Li, G. V. Korshin, *Environ. Sci. Technol.* **2001**, 35, 4905.
- [21] E. Van Achterbergh, C. G. Ryan, S. E. Jackson, W. L. Griffin in *Laser-Ablation-ICP-MS in the Earth Sciences*, Mineralogical Association of Canada, Shortcourse, **2001**, p. 239.
- [22] S. Seifert, R. E. Winans, D. M. Tiede, P. Thiyagarajan, *J. Appl. Crystallogr.* **2000**, 33, 782.
- [23] P. Thiyagarajan, F. Zeng, C. Y. Ku, S. C. Zimmerman, *J. Mater. Chem.* **1997**, 7, 1221.
- [24] P. Thiyagarajan, *J. Appl. Crystallogr.* **2003**, 36, 373.